

<https://doi.org/10.15407/ujpe69.11.781>

P.-C. BOBOC on behalf of the NA62 Collaboration

Horia Hulubei National Institute for R&D in Physics and Nuclear Engineering
(30, Reactorului Str., Măgurele, Romania; e-mail: petre.constantin.boboc@cern.ch)

RECENT RESULTS FROM PRECISION MEASUREMENTS AT THE NA62 EXPERIMENT¹

Experiment NA62 at CERN collected the world's largest dataset of charged Kaons, the main goal being the measurement of the $\mathcal{B}(K^+ \rightarrow \pi^+ \nu \bar{\nu})$. New results from the analyses of rare kaon and pion decays using data samples collected in 2017–2018 are presented. A sample of $K^+ \rightarrow \pi^+ \gamma \gamma$ decays was collected using a minimum-bias trigger and measurement of the branching ratio, study of the di-photon mass spectrum, and the first search for production and prompt decay of an axion-like particle with gluon coupling in the process $K^+ \rightarrow \pi^+ A$, $A \rightarrow \gamma \gamma$ are reported. Additionally, a sample of $\pi^0 \rightarrow e^+ e^-$ decays was collected, using a dedicated scaled down di-electron trigger, and preliminary results for the branching ratio are reported.

Key words: pion decays, kaon decays, chiral perturbation theory.

1. The NA62 Experiment

The NA62 is a fixed target experiment at CERN's SPS North Area which has the goal to measure the branching ratio of the ultra-rare $K^+ \rightarrow \pi^+ \nu \bar{\nu}$ decay [1].

A 400 GeV/c proton beam is extracted from the CERN's Super Proton Synchrotron (SPS) which hits a beryllium target, generating a 75 GeV/c secondary beam consisting of 70% π^+ , 24% protons, and 6% K^+ . The kaons are identified using the KTAG, a Cherenkov detector, while particles in the secondary beam are tracked by the GTK, a silicon pixel beam tracker. These particles travel through the experiment's fiducial decay volume, where kaon decays are reconstructed by measuring the momentum of the charged decay products using the STRAW spectrometer. Particle identification is facilitated by the Ring Imaging Cherenkov (RICH) Detector, the liquid krypton (LKr) calorimeter, and a muon veto system. To veto photons outside the LKr's acceptance, additional systems, including the large-angle (LAV) and small-angle (IRC and SAC) photons detectors

are employed. A schematic view of the NA62 detector is shown in Fig. 1 and more details regarding the apparatus can be found in [2].

Thanks to the multiple trigger lines [3] and the versatility of the experiment, besides the $K^+ \rightarrow \pi^+ \nu \bar{\nu}$, multiple K^+ decays can be studied. Other NA62 recent results are published in [4] and [5].

2. Measurement of the $K^+ \rightarrow \pi^+ \gamma \gamma$ Decay

Experimental studies of radiative kaon decays offer a way to test Chiral Perturbation Theory (ChPT), which describes low-energy QCD processes. In the case of the $K^+ \rightarrow \pi^+ \gamma \gamma$ decay, ChPT has been formulated at both leading and next-to-leading orders, incorporating an unknown real parameter \hat{c} along with other external parameters.

A sample of 3984 $K^+ \rightarrow \pi^+ \gamma \gamma$ decay candidates was selected with an estimated background of 291 ± 14 events [6] using the 2017 and 2018 NA62 dataset with the primary background originating from the $K^+ \rightarrow \pi^+ \pi^0 \gamma$, $\pi^0 \rightarrow \gamma \gamma$ decay, where photons create overlapping showers in the LKr calorimeter, resulting in the reconstruction of merged clusters. The background is estimated using simulations, which are validated by comparing the simulation of cluster merging with a dedicated data sample. The $K^+ \rightarrow \pi^+ \pi^0$, $\pi^0 \rightarrow \gamma \gamma$ decays were used as normalization

Citation: Boboc P.-C. on behalf of the NA62 Collaboration. Recent results from precision measurements at the NA62 experiment. *Ukr. J. Phys.* **69**, No. 11, 781 (2024). <https://doi.org/10.15407/ujpe69.11.781>.

© Publisher PH “Akademperiodyka” of the NAS of Ukraine, 2024. This is an open access article under the CC BY-NC-ND license (<https://creativecommons.org/licenses/by-nc-nd/4.0/>)

¹ This work is based on the results presented at the 2024 “New Trends in High-Energy and Low-x Physics” Conference.

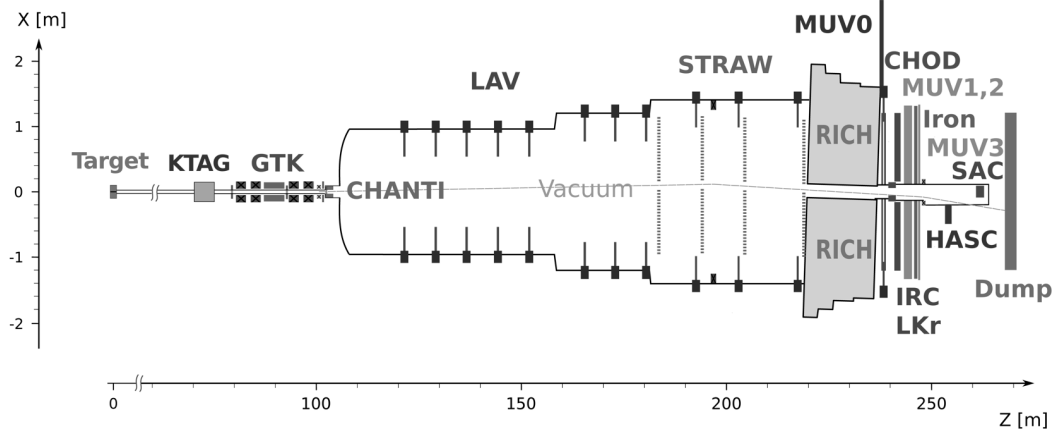


Fig. 1. Schematic side view of the NA62 beam line and detector used in 2018

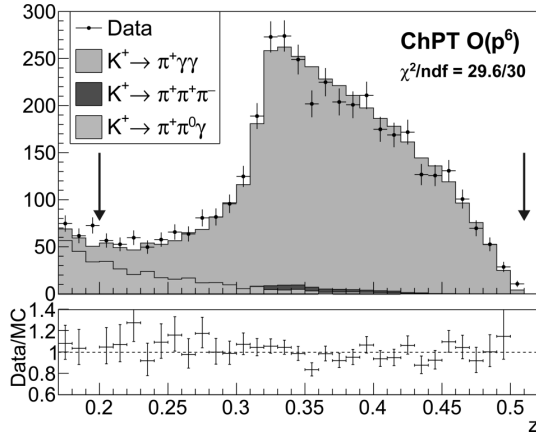


Fig. 2. Reconstructed z spectrum of the $K_{\pi\gamma\gamma}$ candidates, estimated background contributions and simulated signal spectra in ChPT $\mathcal{O}(p^6)$ description

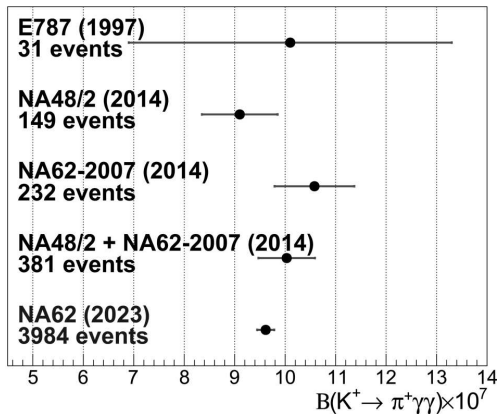


Fig. 3. Summary of \mathcal{B} measurement in ChPT $\mathcal{O}(p^6)$ framework

sample. Fits of the observable $z = m_{\gamma\gamma}^2/m_K^2$ to the data were performed for both leading order $\mathcal{O}(p^4)$ and next-to-leading order $\mathcal{O}(p^6)$ ChPT descriptions where the p-values obtained from the fit are 2.7×10^{-8} and 0.49, respectively indicating that the next-to-leading order contribution in ChPT is necessary to describe the di-photon invariant mass, seen in Fig. 2.

The value of \hat{c} obtained in ChPT $\mathcal{O}(p^6)$ is $\hat{c} = 1.144 \pm 0.069_{\text{stat}} \pm 0.034_{\text{syst}}$. By integration the ChPT $\mathcal{O}(p^6)$ branching ratio in the full kinematic range, the corresponding branching ratio is $\mathcal{B} = (9.61 \pm 0.15_{\text{stat.}} \pm 0.07_{\text{syst.}}) \times 10^{-7}$. In the region $z \in (0.2, 0.51)$, by summing over the z bins, the model independent branching ratio is $\mathcal{B}_{\text{MI}}(z > 0.2) = (9.46 \pm 0.19_{\text{stat.}} \pm 0.07_{\text{syst.}}) \times 10^{-7}$. The comparison between the branching ratio obtained from ChPT $\mathcal{O}(p^6)$ and previous measurements can be seen in Fig. 3.

The differential $K_{\pi\gamma\gamma}$ decay width as function of z spectrum corresponding to $\hat{c} = 1.144$ obtained from the model-independent measurement is displayed in Fig. 4. A first search for an axion-like particle (ALP) a in the decay channel $K^+ \rightarrow \pi^+ a, a \rightarrow \gamma\gamma$ was conducted using the same selected event sample. A peak search was performed across 287 mass hypotheses in the range of 207–350 MeV/c^2 , with mass steps of 0.5 MeV/c^2 and a resolution for m_a varying between 2.0 MeV/c^2 and 0.2 MeV/c^2 . For each hypothesis on m_a , the background was estimated via simulations. Upper limits on the number of signal events and the corresponding branching ratio (under the assumption of prompt $a \rightarrow \gamma\gamma$ decay) were determined using the CL_s method [7], as shown in Fig. 5.

Additionally, in the BC11 scenario, limits are established on the coupling strength of the ALP to gluons ($1/f_G$), show in Figure 6, with the ALP's proper mean lifetime scaling as $\tau_a \sim f_G^2$.

3. Measurement of the $\pi^0 \rightarrow e^+e^-$ Decay

The primary objective in studying the decay $\pi^0 \rightarrow e^+e^-$ is to determine its branching ratio.

Experimentally, additional radiative photons may appear in the final state, meaning that the observable branching ratio includes final-state radiation, making radiative corrections essential for accurate analysis. To account for this, a kinematic variable, $x = m_{ee}^2/m_\pi^2$ which is related to the di-electron invariant mass is defined. Therefore, the measured branching ratio is $\mathcal{B}(\pi^0 \rightarrow e^+e^-(\gamma), x > x_{\text{cut}})$, where the chosen value of x_{cut} must be sufficiently large to suppress the contribution from the Dalitz decay, $\pi^0 \rightarrow e^+e^-\gamma$, which dominates at low x . For $x_{\text{cut}} = 0.95$, the partial Dalitz decay branching ratio accounts for about 3.3% of $\mathcal{B}(\pi^0 \rightarrow e^+e^-(\gamma))$.

The previous best measurement, from the KTeV-E799-II experiment [8], reported $\mathcal{B}_{\text{KTeV}}(\pi^0 \rightarrow e^+e^-(\gamma), x > 0.95) = (6.44 \pm 0.25 \pm 0.28) \times 10^{-8}$. Using the latest radiative corrections [9, 10] and extrapolating to obtain the branching ratio without final-state radiation, the result

$$\mathcal{B}_{\text{KTeV}}(\pi^0 \rightarrow e^+e^-, \text{no-rad}) = (6.84 \pm 0.35) \times 10^{-8}$$

was obtained, showing a 2σ discrepancy with the most recent theoretical prediction of $\mathcal{B}_{\text{th}}(\pi^0 \rightarrow e^+e^-, \text{no-rad}) = (6.25 \pm 0.03) \times 10^{-8}$ [11].

For this measurement, NA62 utilized data samples from 2017 and 2018, selecting the decay $K^+ \rightarrow \pi^+\pi^0, \pi^0 \rightarrow e^+e^-$, which incorporates the latest radiative corrections in the Monte Carlo simulations with the $K^+ \rightarrow \pi^+e^+e^-$ decay used for normalization.

A dedicated multi-track electron trigger line, which was reduced by a factor of 8, was implemented to collect both $K^+ \rightarrow \pi^+\pi^0, \pi^0 \rightarrow e^+e^-$ and $K^+ \rightarrow \pi^+e^+e^-$ events, resulting in an overall trigger efficiency of approximately 90% for both the signal and normalization selections. With both the signal and normalization decay modes having identical final states, the cancellation of several systematic effects is achieved.

The selection criteria for signal and normalization events are as follows: a three-track vertex topology

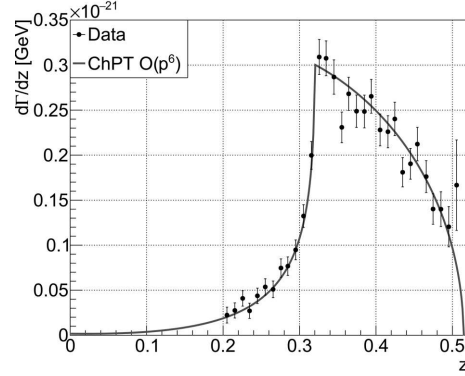


Fig. 4. $d\Gamma/dz$ as function of z . The markers represent the model independent measurements in the signal region and the solid line represents the differential decay width in ChPT $\mathcal{O}(p^6)$ framework

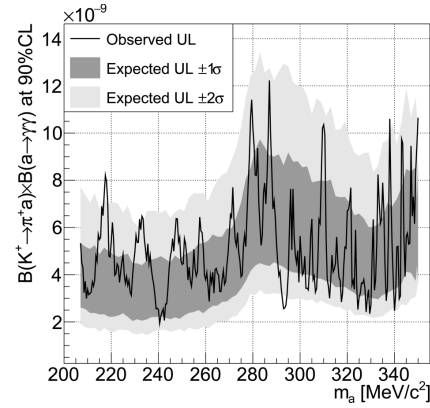


Fig. 5. $\mathcal{B}(K^+ \rightarrow \pi^+ a) \times \mathcal{B}(a \rightarrow \gamma\gamma)$ upper limits at 90% CL with their expected bands assuming prompt ALP decays

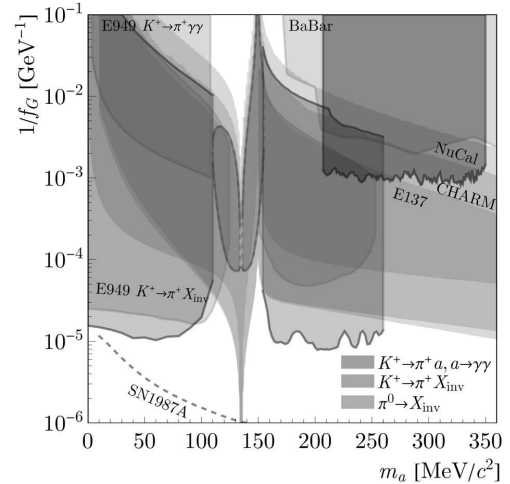


Fig. 6. Exclusion regions at 90% CL in the BC11 scenario parameter space ($m_a, 1/f_G$)

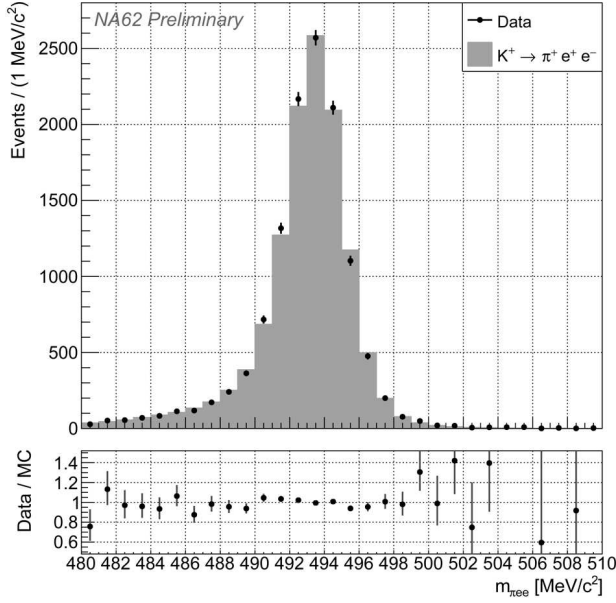


Fig. 7. m_{ee} distribution for candidates satisfying the normalization conditions

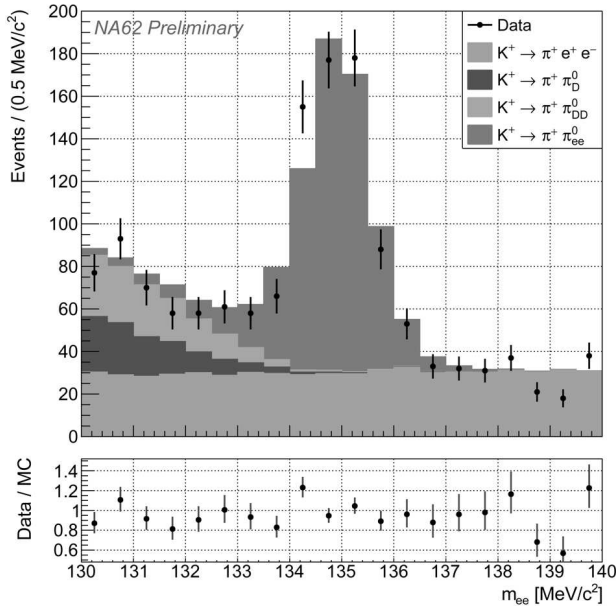


Fig. 8. m_{ee} distribution for signal selection

must be established using data from the STRAW, along with kinematic constraints on the total and transverse momenta of the vertex, and time coincidence information from the CHOD and KTAG detectors.

Track identification is achieved through the energy deposited in the LKr (E) and the momentum measured by the STRAW (p). Specifically, an $E/p < 0.9$ requirement is imposed for the π^+ tracks, while an E/p condition in the interval of $(0.9, 1.1)$ is applied for the e^\pm tracks. For signal events, the dielectron invariant mass, m_{ee} , must fall within the interval of $(130, 140)$ MeV/c^2 , whereas for normalization events, the interval is set to $(140, 360)$ MeV/c^2 . Additionally, the total invariant mass, $m_{\pi ee}$, is required to be between $(480, 510)$ MeV/c^2 (see Fig. 7).

For the normalization sample a negligible background was achieved ($>99.9\%$ sample purity) while for the signal sample the following backgrounds are present:

- $K^+ \rightarrow \pi^+ e^+ e^-$ which is irreducible and flat in the signal region, close the π^0 mass;
- $K^+ \rightarrow \pi^+ \pi^0, \pi^0 \rightarrow e^+ e^- \gamma$ caused by either the irreducible large x-tail of the π^0 Dalitz decay or by photon conversion in the STRAW with an e^\pm track selected from the conversion, in the photon conversion case STRAW hit information is employed to suppress the background;
- $K^+ \rightarrow \pi^+ \pi^0, \pi^0 \rightarrow \pi^+ e^+ e^- e^+ e^-$ where two e^\pm tracks are not reconstructed. Events with a track segment reconstructed in the first two STRAW chambers compatible with the vertex are rejected to suppress this background.

A total of 12,160 normalization candidates were selected, with an acceptance of $A(K^+ \rightarrow \pi^+ e^+ e^-) = (4.70 \pm 0.01_{\text{stat}})\%$ based on simulations. The effective number of kaon decays is calculated to be $N_K = (8.62 \pm 0.08_{\text{stat}} \pm 0.26_{\text{ext}}) \times 10^{11}$, where the external uncertainty arises from the limited precision of the normalization branching ratio, $\mathcal{B}(K^+ \rightarrow \pi^+ e^+ e^-) = (3.00 \pm 0.09) \times 10^{-7}$ [12].

The signal acceptance for $x_{\text{true}} > 0.95$ is $A(K^+ \rightarrow \pi^+ \pi^0, \pi^0 \rightarrow e^+ e^-) = (5.72 \pm 0.02_{\text{stat}})\%$.

The preliminary branching ratio determined is $\mathcal{B}_{\text{NA62}}(\pi^0 \rightarrow e^+ e^- (\gamma), x > 0.95) = (5.86 \pm 0.30_{\text{stat}} \pm 0.11_{\text{syst}} \pm 0.19_{\text{ext}}) \times 10^{-8}$, obtained through a maximum likelihood fit of the Monte Carlo samples to the m_{ee} spectrum observed in the data, with the branching ratio as the parameter of interest (Fig. 8). The signal event yield derived from the fit is 597 ± 29 events.

The preliminary results can be extrapolated to $\mathcal{B}_{\text{NA62}}(\pi^0 \rightarrow e^+ e^-, \text{no-rad}) = (6.22 \pm 0.39) \times 10^{-8}$ using the most recent radiative corrections. The pre-

cision of the NA62 measurement is comparable to that of the KTeV-E799-II experiment, and the two results are in agreement. However, the central value of the NA62 preliminary result is lower and aligns more closely with theoretical predictions.

The precision of the $\mathcal{B}(\pi^0 \rightarrow e^+e^-)$ measurement is expected to improve as NA62 continues data collection until CERN's Long Shutdown 3. Furthermore, a new measurement of $K^+ \rightarrow \pi^+e^+e^-$ is planned using the data collected by NA62, with the goal of increasing the precision of the $\mathcal{B}(K^+ \rightarrow \pi^+e^+e^-)$ measurement and, thus, reducing the external uncertainties.

1. E.C. Gil *et al.* Measurement of the very rare $K^+ \rightarrow \pi^+\nu\bar{\nu}$ decay. *J. High Energy Phys.* **6**, 93 (2021).
2. E.C. Gil *et al.* The beam and detector of the NA62 experiment at CERN. *J. Instrumentation* **12**, P05025 (2017).
3. E.C. Gil *et al.* Performance of the NA62 trigger system. *J. High Energy Phys.* **3**, 122 (2023).
4. E.C. Gil *et al.* A study of the $K^+ \rightarrow \pi^+0 \rightarrow e^+e^- \gamma\gamma$ decay. *J. High Energy Phys.* **9**, 40 (2023).
5. E.C. Gil *et al.* A measurement of the $K^+ \rightarrow \pi^+\mu^+\mu^-$ decay. *J. High Energy Phys.* **11**, 11 (2022).
6. E. Cortina Gil *et al.* Measurement of the $K^+ \rightarrow \pi^+\gamma\gamma$ decay. *Phys. Lett. B* **850**, 138513 (2024).
7. A.L. Read. Presentation of search results: the CL_s technique. *J. Phys. G: Nucl. Part. Phys.* **28**, 2693 (2002).
8. E. Abouzaid *et al.* Measurement of the rare decay $\pi^0 \rightarrow e^+e^-$. *Phys. Rev. D* **75**, 012004 (2007).
9. T. Husek, K. Kampf, J. Novotný. Rare decay: On corrections beyond the leading order – EPJ C. *Euro. Phys. J. C* **74**, (2014).

10. P. Vaško, J. Novotný. Two-loop QED radiative corrections to the decay $\pi^0 \rightarrow e^+e^-$: The virtual corrections and soft-photon bremsstrahlung. *J. High Energy Phys.* **10**, 122 (2011).
11. M. Hoferichter *et al.* Open Access Improved standard-model prediction for $\pi^0 \rightarrow e^+e^-$. *Phys. Rev. Lett.* **128**, 172004 (2022).
12. S. Navas *et al.* Review of particle physics. *Phys. Rev. D* **110**, 030001 (2024).

Received 20.10.24

П.-Ц. Бобок від імені колаборації NA62

ОСТАННІ РЕЗУЛЬТАТИ ТОЧНИХ ВИМІРЮВАНЬ НА ЕКСПЕРИМЕНТІ NA62

Експеримент NA62 у CERN зібрав найбільшу у світі базу даних про заряджені каони, причому головною метою було вимірювання $\mathcal{B}(K^+ \rightarrow \pi^+\nu\bar{\nu})$. В цій роботі представлено нові результати аналізу рідкісних розпадів каонів і піонів з використанням даних, зібраних у 2017–2018 роках. Ми обговорюємо приклади розпадів $K^+ \rightarrow \pi^+\gamma\gamma$, які було зафіксовано за допомогою тригера мінімального зміщення та вимірювання коефіцієнта розгалуження, досліджуємо масовий спектр подвійних гамма-квантів, проводимо перший пошук можливості утворення і швидкого розпаду аксіоноподібної частинки з глюонним зв'язком у процесі $K^+ \rightarrow \pi^+A, A \rightarrow \gamma\gamma$. Крім того, було зафіксовано розпад $\pi^0 \rightarrow e^+e^-$ за допомогою спеціального діелектронного тригера, і ми наводимо попередні результати щодо коефіцієнта розгалуження.

Ключові слова: розпади піонів, розпади каонів, хіральна теорія збурень.